Theor Chim Acta (1992) 84: 1–19

Theoretica Chimica Acta

© Springer-Verlag 1992

Quantum field theoretical methods in chemically bonded systems II

Diagrammatic perturbation theory*

Thomas E. Sorensen[1], Walter B. England[1], David M. Silver[2], and E. Otto Steinborn[3]

[1] Department of Chemistry and Laboratory for Surface Studies, University of Wisconsin-Milwaukee, Milwaukee, WI 53201, USA

[2] Applied Physics Laboratory, Johns Hopkins University, Laurel, MD 20723, USA

[3] Institut für Physikalische und Theoretische Chemie, Universität Regensburg, W-8400 Regensburg, Germany

Received May 23, 1991/Accepted December 20, 1991

Summary. Many-body perturbation theory is derived for chemical bonds. Paired quasiparticles represent the bonds. Products of the paired quasiparticles define a model Bardeen–Cooper–Schrieffer function. The pairing force is added as a model interaction to the self-consistent problem. The starting model is based on valency and adiabatic symmetry correlation. Symmetries are enforced by the model Hamiltonian. Perturbative corrections are expressed as ordinary Feynman diagrams. The number of diagrams needed is the same as for particle-hole theory.

PACS number(s) 31.10. + z, 71.10. + x, 31.15. + q

Key words: Perturbation theory – Quasiparticles – Feynman diagrams

1. Introduction

Perturbation theory is an approximation strategy based on the belief that differences between solvable models of physical systems and real physical systems are small and continuous. It is formulated as an infinite series of powers of these differences. A finite number of terms may yield an excellent approximation, but it cannot necessarily be applied systematically to arbitrary accuracy. The most that can be asked of applications is that the perturbative series converges.

Perturbation theory for many-body systems yields an infinite expansion in the many-particle interaction. Unfortunately, in most real many-particle systems, the interaction between particles is not small. The Fermi energy, the interaction potential, the range of the interaction and the particle density are all of order unity in atomic units. There is not a convenient small parameter with which to develop a perturbation theory as an expansion in this parameter.

* This work was supported in part by the U.S. Department of the Navy, Space and Naval Warfare Systems Command under Contract N00039-89-C-0001, and in part by NATO Research Grant 1861. It was presented, in part, at the A.C. Wahl Memorial Session, Molecular Spectroscopy Symposium, Columbus, Ohio, 1984; and Midwest Theoretical Chemistry Conference, Milwaukee, Wisconsin, 1985.

Quantized many-body systems may be described with quasiparticles and elementary excitations which interact weakly compared to bare particles and fields. Model solutions show how one passes from strong basic interactions between bare particles to weak residual interactions between quasiparticles [1, pp 2–3]. In this way, many-body problems have been successfully dealt with by replacing the actual system with a perturbative approach that uses an appropriate system of quasiparticles, and it is believed that this approach at least applies to low-lying states [2, p 2].

A reasonable system of quasiparticles to use as a starting point is one which gives a realistic single-particle description. A unified theory has developed which is formulated as a simple (but nontrivial) extension of ordinary nonrelativistic one-particle quantum theory [3, p vii], called many-body perturbation theory (MBPT). The single-particle levels make up a *physical vacuum.* Interactions occur relative to this vacuum and are represented by nonredundant scattering diagrams known as Feynman diagrams (FD). FD constitute an exact order-by-order series expansion for the many-body system. Up to any order, and relative to the physical vacuum, the sum of all FD corresponding to this order-by-order series scales correctly against extensive parameters of the system.

Model building is at the logical core of applications [4, p 5]. Model building in small systems is not particularly difficult: Unless the starting point is chosen with "deliberate stupidity", as for example with the wrong symmetry, "almost any starting point can be moved in the general direction of reality by judicious improvement" [4, p 125]. This is supported by experience with variational methods and low-lying electronic states of most atoms and molecules. It is also supported by MBPT when applied to appropriate problems. A point of confusion arises because sometimes starting models that break symmetry are used for applications of MBPT, and these appear to fall in the category of deliberate stupidity.

Nevertheless, it is often convenient to choose a starting model for MBPT which breaks one or more symmetries [5, p 429]. Consequences depend on the symmetry which is violated. For example, translational symmetry is usually broken without observable consequences in finite problems. Symmetries such as particle-number or angular momentum must usually be maintained. There are general methods for enforcing needed symmetries [6, Chaps. 10 and 11], [5, Chap. 8]. *Perturbative corrections will not restore a broken symmetry unless an appropriate infinite number of FD is summed* [5, p 431].

The full apparatus of MBPT is applicable for studies of *Fermi liquids* [4, p 107]. Two general classes of single-particle starting models are available: *normal* and *superfluid.* Normal models are those with localized quasiparticle interactions [7, p 87]. Hartree–Fock (HF) theory is a normal model [5, Sect. 10.3]. The physical vacuum is a determinant and quasiparticles are called particles and holes [8, Sect. 11.3]. HF effective potentials are sums of direct (Hartree) and exchange (Fock) potentials. The internal propagators of the FD describe particles and holes. When a HF starting model is realistic and appropriate, MBPT is capable of describing the main features of electron correlation in finite systems [8, p 282].

Superfluid models are those with bound states connecting two particles or two holes [7, p 111]. Particle-hole levels become fractionally occupied. The model interactions which describe the bound states are called *pairing interactions.* The model physical vacuum is a Bardeen–Cooper–Schrieffer (BCS) function [7, Eq. (7-14)]. Effective potentials or mean fields for superfluids are sums of Hartree,

Fock and pairing potentials. The internal propagators of the FD describe quasiparticles which are uncoupled relative to the HF and pairing potentials. Propagators of this type can lead to *double counting* – counting some FD two times, always a danger in diagram games [4, p 124].

Single-determinantal or normal starting models of chemical bonds almost always break symmetry. The true ground state cannot be connected adiabatically to a single determinant. If proper symmetry is not included in the model, angular momentum may not be conserved or incorrect charges may be assigned to fragments. MBPT can diverge for certain ranges of parameters. However, inclusion of proper symmetry in the normal starting model is straightforward [9].

Chemical bonds mix particle levels with hole levels at bond distances where they are degenerate or nearly degenerate. This mixing can be described by superfluid starting models [10–13]. Levels to be mixed may be identified with valency models and adiabatic symmetry correlation diagrams. The BCS function and pairing interactions are set up for the degenerate levels. Hartree and exchange potentials and the model pairing potential define the self-consistent problem. In the language of diagram summation, the infinite self-energy summation for the pairing interaction includes symmetries broken by the normal starting model. Lipkin's method [14] is used to include symmetries broken by the BCS function. Particle-number [10] or angular momentum [15] symmetries may be included.

The general model is called BCSLN [16]. BCS labels the self-consistent vacuum and L refers to Lipkin. N is a reference to Nogami for the method used to include particle-number conservation [17]. Specific models are called BCSLN-M [18]. M labels the model valency and adiabatic correlation diagram used to include symmetry. For example, BCSLN-HL is the superfluid starting point for the self-consistent Heitler–London model.

In the present paper, details of the BCSLN formalism are given. Section 2 describes new aspects of the perturbative method. Section 3 translates these ideas into diagrammatic form. Section 4 provides a conclusion.

Numerical applications of the BCSLN scheme have been presented in a previous letter [16], which is Part I of this series. In that paper, BCSLN has been used to compute binding-energy curves for five diatomic reactions:

$$\left.\begin{aligned} H_2(X^1\Sigma_g^+) &\rightarrow 2H(^2S) \\ LiH(X^1\Sigma^+) &\rightarrow Li(^2S) + H(^2S) \\ FH(X^1\Sigma^+) &\rightarrow F(^2P) + H(^2S) \\ F_2(X^1\Sigma_g^+) &\rightarrow 2F(^2P) \\ N_2(X^1\Sigma_g^+) &\rightarrow 2N(^4S) \end{aligned}\right\}. \tag{1}$$

Each calculation starts with the simplest model which maintains the right symmetries (BCSLN-HL). Each starting bond mixes one particle level with one hole level. Most BCS functions are sums of four determinants for each bond and model Hamiltonians have two (three) parameters for single (multiple) bonds. The additional parameter for the multiple bond provides angular momentum symmetry broken by the Heitler–London model. Satisfactory results are found by third order. F_2 with six lone pairs and N_2 with a triple bond are stringent tests of computational methods. The conclusion is that MBPT which starts from valency models which maintain correct symmetries can solve difficult molecular problems.

2. Perturbative method

2.1. Special quasiparticles

The special Bogoliubov–Valatin (B–V) transformation [6, Eq. (7.12)] mixes particles and holes to yield second-quantized solutions for the pairing interaction:

$$\left.\begin{aligned}\hat{\alpha}_k &= u_k \hat{a}_k - v_k \hat{a}_{\bar{k}}^+ \\ \hat{\alpha}_{\bar{k}} &= u_k \hat{a}_{\bar{k}} + v_k \hat{a}_k^+\end{aligned}\right\} k > 0 \quad \text{and} \quad \bar{k} = -k \text{ are } \textbf{paired} \tag{2}$$

where u_k, v_k are expansion coefficients and $\hat{a}_k^+$ and $\hat{a}_k$ are creation and annihilation operators, respectively. The B–V transformation preserves anticommutation relations and defines a physical vacuum [6, Eq. (6.66)]:

$$\hat{\alpha}_k | - \rangle = 0, \quad \text{for all } k. \tag{3}$$

Coupled quasiparticles are used to set up the starting model. They are defined by a particular special transformation and will be called *special quasiparticles*. For most chemical bonds, $\bar{k}$ has spin opposite to k. Spin-pairing is used in this paper. Other 1-particle quantum numbers such as linear momentum or orbital or total angular momentum may be paired.

The annihilation operators $\hat{a}_k$ are model *canonical* operators. They satisfy anticommutation relations and annihilate the bare vacuum $|\ \rangle$:

$$\hat{a}_k |\ \rangle = 0, \quad \text{for all } k. \tag{4}$$

The 1-particle states ϕ_k associated with the $\hat{a}_k$ are expansion coefficients for the field operator:

$$\hat{\psi}(x) = \sum_k \phi_k(x) \hat{a}_k. \tag{5}$$

The model canonical representation must be defined so that the 1-particle density matrix is diagonalized and the pairing matrix (pairing tensor) has *canonical form* with respect to the physical vacuum [6, p 248]. Conditions may be expressed with special transformation coefficients [19, Eq. (11.54)]:

$$\left.\begin{aligned}\langle - | \hat{a}_k^+ \hat{a}_l | - \rangle &= \delta_{kl} v_k^2, \textbf{ density matrix} \\ \langle - | \hat{a}_k^+ \hat{a}_l^+ | - \rangle = \langle - | \hat{a}_l \hat{a}_k | - \rangle &= \delta_{\bar{k}l} u_k v_k = -\delta_{k\bar{l}} u_l v_l, \textbf{ pairing matrix}\end{aligned}\right\}. \tag{6}$$

The pairing matrix measures particle-hole mixing. $u_k (v_k)$ measures the degree to which ϕ_k is empty (filled) in the physical vacuum. The normalization condition is:

$$u_k^2 + v_k^2 = 1. \tag{7}$$

Conservation of average particle-number n_0 in the physical vacuum is expressed by the sum of 1-particle density-matrix elements:

$$\sum_k v_k^2 = n_0. \tag{8}$$

2.1.1. Model pairs and core levels. Model pairs are starting models for chemical bonds. Core levels are *nonbonded levels*. To set up the models, canonical labels are assigned to subsets F' (*filled levels*), P' (*paired levels*) and E' (*empty levels*).

$$\left.\begin{aligned} F' &= F \cup \bar{F}; \quad F = -\bar{F} = \{q > 0 : v_q^2 \equiv 1\} \\ P' &= P \cup \bar{P}; \quad P = -\bar{P} = \{q > 0 : 0 \leqslant v_q^2 \leqslant 1\} \\ E' &= E \cup \bar{E}; \quad E = -\bar{E} = \{q > 0 : v_q^2 \equiv 0\} \end{aligned}\right\}. \tag{9}$$

Primed subsets count spin-up and spin-down. Barred (unbarred) subsets count spin-down (spin-up).

F' (E') is a subset of labels which map one-to-one onto hole (particle) labels of the single-determinantal (normal) problem. F describes the *model core*:

$$\hat{K} = \prod_{i \in F} \hat{\alpha}_i \hat{\alpha}_{\bar{i}} = \prod_{i \in F} \hat{a}_i^+ \hat{a}_{\bar{i}}^+ . \tag{10}$$

The subset of paired labels P is covered by pairs of subsets h_I and p_I whose labels map one-to-one onto subsets of hole (h_I) and particle (p_I) labels of the normal problem:

$$P = \bigcup_I \{h_I \cup p_I\}. \tag{11}$$

For each value of I, members of h_I and p_I label particles and holes mixed by the starting model for bond I. This defines a *model pair*:

$$\hat{M}_I = \prod_{i \in h_I} \left(\frac{\hat{\alpha}_i \hat{\alpha}_{\bar{i}}}{v_i} \right) \prod_{a \in p_I} \left(\frac{\hat{\alpha}_a \hat{\alpha}_{\bar{a}}}{v_a} \right). \tag{12}$$

There is a conservation condition for the average particle-number assigned to each model pair:

$$\sum_{i \in h_I} v_i^2 + \sum_{a \in p_I} v_a^2 = \frac{n_{I,0}}{2} \tag{13}$$

Distinct model pairs are separated:

$$h_I \cap h_J = p_I \cap p_J = \varnothing, \quad \text{for } \hat{M}_I \neq \hat{M}_J. \tag{14}$$

The labels of Eqs. (9) and (11) are set up once-for-all.

Unperturbed function. The unperturbed function is generated by the product of model core and model pair operators:

$$|-\rangle = \hat{K} \prod_I \hat{M}_I | \; \rangle. \tag{15}$$

$|-\rangle$ is a model canonical BCS function. It is also a model physical vacuum which satisfies the annihilation condition (3). It is assumed that $|-\rangle$ satisfies a variational principle so that there is no additional loss of generality associated with restriction of Eqs. (10) and (12) to binary products of quasiparticle operators with barred and unbarred indices [6, Sect. 7.2.1].

Unperturbed function for two quasiparticles [10]. Two special quasiparticles are paired to describe the Heitler–London model of a bond. Suppose the hole and

particle mixed by the bond are labelled by 1 and 2, respectively. Quasiparticles are also labelled by 1 and 2:

$$h = 1; \quad p = 2; \quad P = \{1, 2\}. \tag{16}$$

The special transformation is:

$$\left.\begin{aligned} \hat{\alpha}_1 &= u_1 \hat{a}_1 - v_1 \hat{a}_{\bar{1}}^+ \quad \hat{\alpha}_2 = u_2 \hat{a}_2 - v_2 \hat{a}_{\bar{2}}^+ \\ \hat{\alpha}_{\bar{1}} &= u_1 \hat{a}_{\bar{1}} + v_1 \hat{a}_1^+ \quad \hat{\alpha}_{\bar{2}} = u_2 \hat{a}_{\bar{2}} + v_2 \hat{a}_2^+ \end{aligned}\right\}. \tag{17}$$

The condition for average particle-number conservation is:

$$v_1^2 + v_2^2 = 1. \tag{18}$$

The BCS function is a sum of four determinants:

$$|-\rangle = u_1 u_2 |0\rangle + v_1 v_2 |4\rangle + (v_1 u_2 \hat{a}_1^+ \hat{a}_{\bar{1}}^+ + u_1 v_2 \hat{a}_2^+ \hat{a}_{\bar{2}}^+)| \ \rangle. \tag{19}$$

$|0\rangle$ and $|4\rangle$ are determinantal wave functions for zero and four quasiparticles, respectively:

$$|0\rangle = | \ \rangle, \quad |4\rangle = \hat{a}_1^+ \hat{a}_{\bar{1}}^+ \hat{a}_2^+ \hat{a}_{\bar{2}}^+ | \ \rangle. \tag{20}$$

Conditions are needed before the remaining terms can be related to a specific wave function.

Suppose the exact model wave function for the ground state is:

$$|2\rangle = (|C_1| \hat{a}_1^+ \hat{a}_{\bar{1}}^+ - |C_2| \hat{a}_2^+ \hat{a}_{\bar{2}}^+)| \ \rangle, \qquad C_1^2 + C_2^2 = 1. \tag{21}$$

A model BCS function may be defined by two conditions on the special transformation coefficients:

$$v_1 = u_2 = [|C_1|/(|C_1| + |C_2|)]^{1/2}; \qquad u_1 = -v_2 = [|C_2|/(|C_1| + |C_2|)]^{1/2}. \tag{22}$$

This model BCS function is equivalent to the exact model wave function for the ground state:

$$|-\rangle = (|C_1| + |C_2|)^{-1}[|C_1||C_2|(|0\rangle - |4\rangle) + |2\rangle]. \tag{23}$$

2.2. Model Hamiltonian and L operators

The general formula for the model Hamiltonian $\hat{H}_L$ is:

$$\hat{H}_L = \hat{H} - \hat{f}_0 - \hat{f}_1 - \hat{f}_2. \tag{24}$$

$\hat{H}$ is the ordinary Hamiltonian and the $\hat{f}_p$ are normally ordered p-body model operators called *L operators* (for Lipkin). The role of L operators is to enforce desired symmetries, usually with Lipkin's method [14]. Normal ordering is defined with respect to the BCS function [19, Sect. 11.4]. It is denoted by placing strings of operators between colons.

2.2.1. L operators for the Nogami-type Hamiltonian [10], [18]. The Nogami-type model Hamiltonian is a quadratic expansion in the number operator:

$$\hat{H}_L = \hat{H} - \lambda_1(\hat{N} - n_0) - \tfrac{1}{2}\lambda_2(\hat{N} - n_0)^2. \tag{25}$$

$\hat{N}$ is the number operator for paired levels:

$$\hat{N} = \sum_{i \in P} \hat{a}_i^+ \hat{a}_i. \tag{26}$$

The λ_p are parameters whose values are determined to enforce the right symmetries. λ_2 (λ_1) is chosen so that the model energy (model particle-number) has the desired value. Wick's theorem yields the L operators:

$$\hat{f}_0 = \lambda_2 \sum_{k \in P'} u_k v_k \tag{27}$$

$$\left.\begin{aligned} \hat{f}_1 = \lambda : \hat{N} : - \sum_{k \in P'} [\lambda_2 v_k^2 : \hat{a}_k^+ \hat{a}_k : - \tfrac{1}{4}\lambda_2 u_k v_k (: \hat{a}_k^+ \hat{a}_{\bar{k}}^+ : + : \hat{a}_{\bar{k}} \hat{a}_k :)] \\ \lambda = \lambda_1 + \tfrac{1}{2}\lambda_2 \end{aligned}\right\} \tag{28}$$

$$\hat{f}_2 = \tfrac{1}{2}\lambda_2 : \hat{N}^2 : \tag{29}$$

λ is the vestige of the chemical potential. It satisfies a gap equation and may be used to fix the model particle-number. In this case, λ_1 is determined indirectly.

Parameters for two quasiparticles. Expressions for parameters are derived from Lipkin's degeneracy conditions.

$$E_n = \langle n | \hat{H} | n \rangle \left\{ \begin{matrix} \lambda_1 = \tfrac{1}{4}(E_4 - E_0), & \lambda_2 = \tfrac{1}{4}(E_4 - 2E_2 + E_0) \\ \langle - | \hat{H}_L | - \rangle = E_2 \end{matrix} \right\}. \tag{30}$$

$|n\rangle$ labels components of the model BCS function in Eq. (23).

Essentially these equations were used for Heitler–London models for the single bonds of Eq. (1) [20]. E_2 is replaced by the self-consistent Heitler–London energy. E_0 (E_4) is replaced by the energy of the determinant with two fewer (extra) quasiparticles.

2.3. *One-body model Hamiltonian and uncoupled quasiparticles*

The one-body model Hamiltonian is a Hartree–Fock–Bogoliubov-type Hamiltonian set up in the canonical basis.

$$\left.\begin{aligned} \hat{H}_{L0} = \sum_{kl} \left(v_{kl} : \hat{a}_k^+ \hat{a}_l : - \frac{\mu_{kl}}{2} : \hat{a}_k^+ \hat{a}_l^+ : - \frac{\mu_{kl}^*}{2} : \hat{a}_k \hat{a}_l : \right) + E^{(1)} \\ E^{(1)} = \langle - | H_L | - \rangle \end{aligned}\right\}. \tag{31}$$

$E^{(1)}$ is the model energy (energy through first order). v is the model self-consistent energy and μ is the model pairing potential. Each is a sum of contributions from the ordinary Hamiltonian (denoted by superscript (0)) and the one-body L operator (denoted by tildes except for the vestige of the chemical potential λ):

$$\left.\begin{aligned} v_{kl} = \epsilon_{kl} + g_{kl} \qquad \mu_{kl} = \mu_{kl}^{(0)} + \tilde{\mu}_{kl} \\ \epsilon_{kl} = \epsilon_{kl}^{(0)} - \lambda \tilde{\delta}_{kl} \qquad g_{kl} = g_{kl}^{(0)} + \tilde{g}_{kl} \\ g_{kl}^{(0)} = \sum_m (V_{kmlm}^{(0)} - V_{kmml}^{(0)}) v_m^2 \qquad \mu_{kl}^{(0)} = \sum_m V_{k\bar{m}m\bar{l}}^{(0)} u_m v_m \\ \tilde{\delta}_{kl} = \delta_{kl}, \quad \text{for } kl \in P' \qquad \tilde{\delta}_{kl} = \tilde{g}_{kl} = \tilde{\mu}_{kl} = 0, \quad \text{for } kl \notin P' \end{aligned}\right\}. \tag{32}$$

$V_{klmn}^{(0)}$ represents the 2-electron interaction:

$$V_{klmn}^{(0)} = e^2 \int dx_1 \int dx_2 \frac{\phi_k^*(x_1)\phi_l^*(x_2)\phi_m(x_1)\phi_n(x_2)}{r_{12}} = [\phi_k \phi_m | \phi_l \phi_n]. \tag{33}$$

The integration includes spin summation. e is the electronic charge and r_{12} is the distance between the electrons.

$\epsilon^{(0)}$ is the sum of the matrix elements of the 1-electron kinetic energy and the electron-nucleus attraction energy. It is a Hückel-type energy. $g^{(0)}$ is the matrix element of a generalized HF effective potential (generalized direct and exchange interactions). $\mu^{(0)}$ mixes particle and hole levels to form starting models for chemical bonds.

There is more or less a division of labor. v must order the levels correctly and μ must maintain correct symmetries. The right starting models of bonds break the right particle-hole symmetries and maintain the right total symmetries of the problem.

Partition of the one-body L operator for two quasiparticles governed by the Nogami-type Hamiltonian. The model BCS function of Eq. (23) for two quasiparticles does not conserve particle-number. Enforcement of particle-number conservation yields the following partition of the one-body L operator [10, 18].

$$\left.\begin{aligned} \lambda &= \tfrac{1}{8}(3E_4 - 2E_2 - E_0) \\ \tilde{g}_{kl} &= -(E_4 - 2E_2 + E_0)\tilde{\delta}_{kl}v_k^2 \\ \tilde{\mu}_{kl} &= \tfrac{1}{16}(E_4 - 2E_2 + E_0)\delta_{kl}v_k u_k \end{aligned}\right\}. \tag{34}$$

2.3.1. Unperturbed Hamiltonian. The one-body model Hamiltonian is diagonalized in the *energy representation*:

$$\hat{H}_{L0} = \sum_k E_k \hat{\beta}_k^+ \hat{\beta}_k + E^{(1)}. \tag{35}$$

To first order, the quasiparticles $\hat{\beta}_k$ are uncoupled and satisfy Heisenberg equations of motion:

$$i\frac{d}{dt}\hat{\beta}_k(t) = E_k \hat{\beta}_k(t). \tag{36}$$

These are the unperturbed equations of motion. The E_k will make up the energy denominators of MBPT.

The transformation from the model canonical representation $\hat{a}_k$ to the energy representation $\hat{\beta}_k$ is a *general* B–V transformation. It may be expressed as two consecutive steps [6, Sect. 7.2.1]. The first step is the special B–V transformation and the representation of the one-body model Hamiltonian in the special basis.

$$\left.\begin{aligned} \hat{H}_{L0} &= \sum_{kl} \kappa_{kl}\hat{\alpha}_k^+ \hat{\alpha}_l + E^{(1)} \\ \kappa_{kl} &= v_{kl}\left(u_k u_l - \frac{k}{|k|}\frac{l}{|l|}v_k v_l\right) - \frac{k}{|k|}\mu_{\bar{k}l}v_k u_l + \frac{1}{|l|}\mu^*_{k\bar{l}}u_k v_l \end{aligned}\right\}. \tag{37}$$

This is the general form when $|-\rangle$ satisfies a variational condition. The second step is a unitary transformation. The transformation matrix is made up of the eigenvectors of the one-body model Hamiltonian in the special basis.

$$\sum_l \kappa_{kl}\gamma_{lm} = \gamma_{km}E_m, \qquad \hat{\beta}_k = \sum_m \gamma^*_{mk}\hat{\alpha}_m. \tag{38}$$

The uncoupled quasiparticles satisfy fundamental anticommutation relations and can be used to generate the physical vacuum:

$$|-\rangle = \prod_{i\in F}\left(\sum_{s>0}\sum_{t>0}\gamma_{is}\gamma_{it}\hat{\boldsymbol{\beta}}_s\hat{\boldsymbol{\beta}}_{\bar{t}}\right)\prod_{k\in P}\left(\frac{1}{v_k}\sum_{q>0}\sum_{r>0}\gamma_{kq}\gamma_{kr}\hat{\boldsymbol{\beta}}_q\hat{\boldsymbol{\beta}}_{\bar{r}}\right)|\ \rangle \tag{39}$$

$$\hat{\boldsymbol{\beta}}_q|-\rangle = 0, \quad \text{all } q. \tag{40}$$

It is convenient to extend Eqs. (9) and (11) to the uncoupled quasiparticles. This is done once-for-all, usually when $|\gamma_{mm}| \approx 1$.

2.4. *Unperturbed excited states*

Excited states of the model physical vacuum are in one-to-one correspondence with excited states of the normal ground state [21, Sect. 7.4.5].

$$\hat{\boldsymbol{\beta}}^+_{a_1}\hat{\boldsymbol{\beta}}^+_{a_2}\cdots\hat{\boldsymbol{\beta}}^+_{a_n}\hat{\boldsymbol{\beta}}^+_{k_1}\hat{\boldsymbol{\beta}}^+_{k_2}\cdots\hat{\boldsymbol{\beta}}^+_{k_n}|-\rangle. \tag{41}$$

a_i (k_i) is restricted to quasiparticle labels which are empty (filled) in the normal state.

2.4.1. Unperturbed excited states for two quasiparticles. Suppose that the quasiparticle operators $\hat{\boldsymbol{\alpha}}$ and $\hat{\boldsymbol{\beta}}$ are identical. A complete set of unperturbed excited states includes states such as:

$$\hat{\boldsymbol{\alpha}}^+_1\hat{\boldsymbol{\alpha}}^+_{\bar{1}}|-\rangle = (-v_1 + u_1\hat{\boldsymbol{a}}^+_1\hat{\boldsymbol{a}}^+_{\bar{1}})\frac{\hat{\boldsymbol{\alpha}}_2\hat{\boldsymbol{\alpha}}_{\bar{2}}}{v_2}|\ \rangle \tag{42}$$

$$\hat{\boldsymbol{\alpha}}^+_2\hat{\boldsymbol{\alpha}}^+_{\bar{2}}|-\rangle = (-v_2 + u_2\hat{\boldsymbol{a}}^+_2\hat{\boldsymbol{a}}^+_{\bar{2}})\frac{\hat{\boldsymbol{\alpha}}_1\hat{\boldsymbol{\alpha}}_{\bar{1}}}{v_1}|\ \rangle \tag{43}$$

$$\hat{\boldsymbol{\alpha}}^+_1\hat{\boldsymbol{\alpha}}^+_{\bar{1}}\hat{\boldsymbol{\alpha}}^+_2\hat{\boldsymbol{\alpha}}^+_{\bar{2}}|-\rangle = (-v_1 + u_1\hat{\boldsymbol{a}}^+_1\hat{\boldsymbol{a}}^+_{\bar{1}})(-v_2 + u_2\hat{\boldsymbol{a}}^+_2\hat{\boldsymbol{a}}^+_{\bar{2}})|\ \rangle \tag{44}$$

$$\hat{\boldsymbol{\alpha}}^+_1\hat{\boldsymbol{\alpha}}^+_{\bar{2}}|-\rangle = \hat{\boldsymbol{a}}^+_1\hat{\boldsymbol{a}}^+_{\bar{2}}|\ \rangle \tag{45}$$

$$\hat{\boldsymbol{\alpha}}^+_2\hat{\boldsymbol{\alpha}}^+_{\bar{1}}|-\rangle = \hat{\boldsymbol{a}}^+_2\hat{\boldsymbol{a}}^+_{\bar{1}}|\ \rangle \tag{46}$$

$$\hat{\boldsymbol{\alpha}}^+_{\bar{1}}|-\rangle = \hat{\boldsymbol{a}}^+_{\bar{1}}\frac{\hat{\boldsymbol{\alpha}}_2\hat{\boldsymbol{\alpha}}_{\bar{2}}}{v_2}|\ \rangle \tag{47}$$

$$\hat{\boldsymbol{\alpha}}^+_1\hat{\boldsymbol{\alpha}}^+_2\hat{\boldsymbol{\alpha}}^+_{\bar{2}}|-\rangle = \hat{\boldsymbol{a}}^+_1(-v_2 + u_2\hat{\boldsymbol{a}}^+_2\hat{\boldsymbol{a}}^+_{\bar{2}})|\ \rangle. \tag{48}$$

Spurious states occur whenever the physical vacuum violates conservation principles [19]. Two of the three states of Eqs. (42)–(44) are spurious. It will be seen in Sect. 2.4.2 that spurious states such as these are excluded in the present method.

2.4.2. Allowed excited states for two quasiparticles. Level 1 (2) is filled (empty) in the normal ground state. The labels for Eq. (41) are

$$\left.\begin{aligned} k_1 &= 1 \qquad a_1 = 2 \\ k_2 &= \bar{1} \qquad a_2 = \bar{2} \end{aligned}\right\}. \tag{49}$$

Seven excited states of the two quasiparticle problem are defined in Eqs. (42)–(48). Others may be generated in the same way up to a total of fifteen. Suppose for simplicity that a and k have different symmetry properties. This leaves a total of seven excited states. If the one-to-one correspondence of Eq. (41) is enforced, only the excited state defined in Eq. (44) survives. This excited

state is unwanted in MBPT because all two-level correlation is included in the unperturbed energy. The conclusion is that none of the excited states are allowed. No spurious states occur.

2.5. *Perturbative interactions*

The perturbation $\hat{V}^{(1)}$ is the difference between the normally ordered 2-electron interaction and the two-body L operator:

$$\left.\begin{aligned}\hat{V}^{(1)} &= \hat{H}_L - \hat{H}_{L0} \\ &= \hat{V}^{(0)} - \hat{f}_2\end{aligned}\right\} \tag{50}$$

$$\hat{V}^{(0)} = \tfrac{1}{2} \sum_{klmn} V^{(0)}_{klmn} : \hat{a}_k^+ \hat{a}_l^+ \hat{a}_n \hat{a}_m : \tag{51}$$

Matrix elements for the two-body L operator represented in the canonical basis:

$$\hat{f}_2 = \tfrac{1}{2} \sum_{klmn \in P'} \tilde{f}_{2;klmn} : \hat{a}_k^+ \hat{a}_l^+ \hat{a}_n \hat{a}_m : \tag{52}$$

For example, matrix elements for the Nogami-type Hamiltonian can be deduced from Eq. (29):

$$\tilde{f}_{2;klmn} = \lambda_2 \tilde{\delta}_{km} \tilde{\delta}_{ln}. \tag{53}$$

Matrix elements for the perturbation may be represented in the canonical basis:

$$V^{(1)}_{klmn} = V^{(0)}_{klmn} - \tilde{f}_{2;klmn}; \qquad \tilde{f}_{2;klmn} = 0, \quad \text{for } klmn \notin P'. \tag{54}$$

There are symmetry requirements for Coulomb and electron-phonon interactions [22, Eq. (7.34a)]:

$$V^{(1)}_{klmn} = V^{(1)}_{\bar{m}\bar{n}\bar{k}\bar{l}} = V^{(1)}_{\bar{m}\bar{l}\bar{k}n} = V^{(1)}_{\bar{k}\bar{n}\bar{m}\bar{l}}. \tag{55}$$

2.5.1. Interactions among uncoupled quasiparticles. $\hat{V}^{(1)}$ which satisfy the symmetry requirements of Eq. (55) can be expanded with Pauli matrices τ_3 [22, Sect. 7-2]:

$$\hat{V}^{(1)} = \tfrac{1}{2} \sum_{klmn > 0} V^{(1)}_{klmn} : \vec{a}_k^+ \tau_3 \vec{a}_m \vec{a}_l^+ \tau_3 \vec{a}_n : \tag{56}$$

The $\vec{a}_k$ are spinor operators:

$$\vec{a}_k^+ = (\hat{a}_k^+, \hat{a}_{\bar{k}}), \quad k > 0. \tag{57}$$

The transformation from the $\hat{a}_k$ to the $\hat{\beta}_q$ may be written as:

$$\vec{a}_k = (u_k + v_k i\tau_2) \sum_{q > 0} \gamma_{kq} \vec{\beta}_q \tag{58}$$

where τ_2 is a Pauli matrix. The transformed perturbation for BCSLN in the energy representation is:

$$\hat{V}^{(1)} = \tfrac{1}{2} \sum_{qrst > 0} (:[\vec{\beta}_q^+ \Gamma_{qs} \vec{\beta}_s \mid \vec{\beta}_r^+ \Gamma_{rt} \vec{\beta}_t] : - : \vec{\beta}_q^+ \langle \Gamma'_{qs} \rangle \vec{\beta}_s \vec{\beta}_r^+ \langle \Gamma'_{rt} \rangle \vec{\beta}_t :). \tag{59}$$

Matrix elements of $\hat{V}^{(0)}$. The first term on the right-hand-side of Eq. (59) represents $\hat{V}^{(0)}$. The spinor matrix Γ_{qs} is a sum of two *charge distributions*

$\Lambda_{qs}(x, x')$ and $\Omega_{qs}(x, x')$, each multiplied times a Pauli matrix:

$$\Gamma_{qs}(x, x') = \Lambda_{qs}(x, x')\tau_3 + \Omega_{qs}(x, x')\tau_1. \tag{60}$$

The charge distributions can be expanded with 1-particle functions:

$$\left.\begin{aligned} \Lambda_{qs}(x, x') &= t_q^*(x)t_s(x') - \lambda_q^*(x)\lambda_s(x') \\ \Omega_{qs}(x, x') &= t_q^*(x)\lambda_s(x') + \lambda_q^*(x)t_s(x') \end{aligned}\right\} \tag{61}$$

$$\left.\begin{aligned} t_q &= \sum_{k>0} \gamma_{kq} u_k \phi_k \qquad \lambda_q = \sum_{k>0} \gamma_{kq} v_k \phi_k \\ t_{\bar{q}} &= \sum_{k>0} \gamma_{kq} u_k \phi_{\bar{k}} \qquad \lambda_{\bar{q}} = \sum_{k>0} \gamma_{kq} v_k \phi_{\bar{k}} \end{aligned}\right\} \quad \text{for } q > 0. \tag{62}$$

The matrix elements needed to represent $\hat{V}^{(0)}$ can be written with Mulliken's notation for 2-electron interactions introduced in Eq. (33):

$$[\Omega_{qs}|\Omega_{rt}] = [t_q\lambda_s|t_r\lambda_t] + [t_q\lambda_s|\lambda_r t_t] + [\lambda_q t_s|t_r\lambda_t] + [\lambda_q t_s|\lambda_r t_t] \tag{63}$$

$$[\Omega_{qs}|\Lambda_{rt}] = [t_q\lambda_s|t_r t_t] - [t_q\lambda_s|\lambda_r\lambda_t] + [\lambda_q t_s|t_r t_t] - [\lambda_q t_s|\lambda_r\lambda_t] \tag{64}$$

$$[\Lambda_{qs}|\Lambda_{rt}] = [t_q t_s|t_r t_t] - [t_q t_s|\lambda_r\lambda_t] - [\lambda_q\lambda_s|t_r t_t] + [\lambda_q\lambda_s|\lambda_r\lambda_t]. \tag{65}$$

t_q (λ_q) is *particle-like* (*hole-like*) when almost empty (filled):

$$\left.\begin{aligned} t_q &\to \phi_q(\textbf{particle}) \\ \lambda_q &\to \phi_q(\textbf{hole}) \end{aligned}\right\} |u_k| \quad \text{and} \quad |v_k| = 1 \text{ or } 0 \text{ for all } k. \tag{66}$$

t_q and λ_q are *equivalent* when the pairing interaction is maximal:

$$t_q \to \pm\lambda_q, \qquad |u_k| = |v_k| = \tfrac{1}{2} \quad \text{for all } k. \tag{67}$$

Equivalence means particles and holes are completely mixed.

Matrix elements of $\hat{f}_2$. The second term on the right-hand-side of Eq. (59) is the representation of $\hat{f}_2$:

$$\langle\Gamma'_{qs}\rangle = \langle\Lambda'_{qs}\rangle\tau_3 + \langle\Omega'_{qs}\rangle\tau_1; \qquad \langle\Lambda'_{qs}\rangle = \langle\Omega'_{qs}\rangle = 0, \quad \text{for } qs \notin P. \tag{68}$$

Three products of model matrix elements are needed to represent $\hat{f}_2$.

$$\langle\Omega'_{qs}\rangle\langle\Omega'_{rt}\rangle; \qquad \langle\Lambda'_{qs}\rangle\langle\Omega'_{rt}\rangle; \qquad \langle\Lambda'_{qs}\rangle\langle\Lambda'_{rt}\rangle. \tag{69}$$

Nogami-type Hamiltonian. Matrix elements follow from Eq. (53).

$$\langle\Omega'_{qs}\rangle = \langle t_q|\lambda_s\rangle + \langle\lambda_q|t_s\rangle; \qquad \langle\Lambda'_{qs}\rangle = \langle t_q|t_s\rangle - \langle\lambda_q|\lambda_s\rangle. \tag{70}$$

$\langle a|b\rangle$ is ordinary bra-ket notation for inner products. Both matrix elements vanish in the particle-hole limit. In the limit of maximal pairing, $\langle\Lambda'_{qs}\rangle$ vanishes and $\langle\Omega'_{qs}\rangle$ becomes $\pm\tilde{\delta}_{qs}$:

$$\left.\begin{aligned} \langle\Omega'_{qs}\rangle &= \langle\Lambda'_{qs}\rangle = 0, \qquad |u_k| \quad \text{and} \quad |v_k| = 1 \text{ or } 0 \quad \text{for all } k \\ \langle\Omega'_{qs}\rangle &= \pm\tilde{\delta}_{qs}, \qquad \langle\Lambda'_{qs}\rangle = 0, \qquad |u_k| = |v_k| = \tfrac{1}{2}, \quad \text{for all } k \end{aligned}\right\}. \tag{71}$$

3. Diagrammatic method

The canonical spinor representation has the form required to make the Feynman–Dyson perturbation series rules work for one- and two-body operators [22, p 174]. In the energy representation, spinor propagators assign charge distributions and model matrix elements to two scattering vertices. Vertices connected by

interaction lines are diagrammatic representatives of the perturbation. Interactions between quasiparticles reduce to differences between two terms. One is an integral over a binary product of charge distributions and the other is one of the binary products for the two-body L operator (Eq. (69)).

3.1. Propagator lines

The time-dependent spinor-matrix propagator is defined by:

$$G_{q\alpha\beta}(t) = i\langle - | T\vec{\beta}_{q\alpha}(t)\vec{\beta}^{+}_{q\beta}(0) | - \rangle \quad \text{for } \alpha, \beta = 1, 2 \tag{72}$$

where T is Wick's time-ordering operator and the components are:

$$\vec{\beta}_{q1} = \hat{\beta}_q \qquad \vec{\beta}_{q2} = \hat{\beta}^{+}_q. \tag{73}$$

Spin-down states are chosen to move backward in time. Spin-up propagation is represented by:

$$G(\uparrow) = i\begin{pmatrix} 1 & 0 \\ 0 & 0 \end{pmatrix} \tag{74}$$

and spin-down propagation by:

$$G(\downarrow) = -i\begin{pmatrix} 0 & 0 \\ 0 & 1 \end{pmatrix}. \tag{75}$$

The propagators are essentially idempotent and satisfy projection relations.

$$\left.\begin{aligned} G(\uparrow)G(\uparrow) = iG(\uparrow); \qquad G(\downarrow)G(\downarrow) = -iG(\downarrow) \\ G(\uparrow)G(\downarrow) = G(\downarrow)G(\uparrow) = 0 \end{aligned}\right\}. \tag{76}$$

3.2. Scattering vertices

Propagators satisfy multiplication rules:

$$G(\uparrow)\tau_3 G(\downarrow) = G(\uparrow)\tau_1 G(\uparrow) = G(\downarrow)\tau_1 G(\downarrow) = 0. \tag{77}$$

The vertices Γ_{qs} and $\langle \Gamma'_{qs} \rangle$ can be replaced by the pairs of vertices $\Omega_{qs}\tau_1$, $\Lambda_{qs}\tau_3$ and $\langle \Omega'_{qs} \rangle \tau_1$, $\langle \Lambda'_{qs} \rangle \tau_3$, respectively:

$$\left.\begin{aligned} G(\uparrow)\Gamma_{qs}G(\downarrow) &= G(\uparrow)\Omega_{qs}\tau_1 G(\downarrow) \\ G(\uparrow)\Gamma_{qs}G(\uparrow) &= G(\uparrow)\Lambda_{qs}\tau_3 G(\uparrow) \\ G(\downarrow)\Gamma_{qs}G(\downarrow) &= G(\downarrow)\Lambda_{qs}\tau_3 G(\downarrow) \end{aligned}\right\} \tag{78}$$

$$\left.\begin{aligned} G(\uparrow)\langle \Gamma'_{qs} \rangle G(\downarrow) &= G(\uparrow)\langle \Omega'_{qs} \rangle \tau_1 G(\downarrow) \\ G(\uparrow)\langle \Gamma'_{qs} \rangle G(\uparrow) &= G(\uparrow)\langle \Lambda'_{qs} \rangle \tau_3 G(\uparrow) \\ G(\downarrow)\langle \Gamma'_{qs} \rangle G(\downarrow) &= G(\downarrow)\langle \Lambda'_{qs} \rangle \tau_3 G(\downarrow) \end{aligned}\right\}. \tag{79}$$

This is represented diagrammatically on Fig. 1. Dark (light) vertices are τ_1-vertices (τ_3-vertices), and are associated with the label $\Omega(\Lambda)$. Unique interactions are identified by connecting scattering vertices with interaction lines

$\mathbf{G}(\uparrow)\Omega_{qr}\tau_3\mathbf{G}(\downarrow)$ or $\mathbf{G}(\uparrow)\langle\Omega'_{qr}\rangle\tau_3\mathbf{G}(\downarrow)$

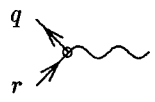

$\mathbf{G}(\uparrow)\Lambda_{qr}\tau_3\mathbf{G}(\uparrow)$ or $\mathbf{G}(\uparrow)\langle\Lambda'_{qr}\rangle\tau_3\mathbf{G}(\uparrow)$

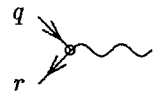

$\mathbf{G}(\downarrow)\Lambda_{qr}\tau_3\mathbf{G}(\downarrow)$ or $\mathbf{G}(\downarrow)\langle\Lambda'_{qr}\rangle\tau_3\mathbf{G}(\downarrow)$

Fig. 1. Scattering vertices

$(\sim\sim\sim\sim)$ in all possible ways:

$$\left.\begin{aligned} \bullet\sim\sim\sim\sim\bullet &\rightarrow (\Omega_{qr}|\Omega_{st}) = [\Omega_{qr}|\Omega_{st}] - \langle\Omega'_{qr}\rangle\langle\Omega'_{st}\rangle \\ \bullet\sim\sim\sim\sim\circ &\rightarrow (\Omega_{qr}|\Lambda_{st}) = [\Omega_{qr}|\Lambda_{st}] - \langle\Omega'_{qr}\rangle\langle\Lambda'_{st}\rangle \\ \circ\sim\sim\sim\sim\circ &\rightarrow (\Lambda_{qr}|\Lambda_{st}) = [\Lambda_{qr}|\Lambda_{st}] - \langle\Lambda'_{qr}\rangle\langle\Lambda'_{st}\rangle \end{aligned}\right\}. \tag{80}$$

3.3. Closed loops

Closed loops are trajectories which begin and end on the same vertex. In a theory where spin-components are degenerate, one expects closed loops such as those shown on Fig. 2 to be equivalent. This will now be demonstrated. Every closed loop has an even number of dark vertices and some number of light vertices. Starting the loop with a dark vertex, those of current interest may be represented by the matrix $\boldsymbol{L}$:

$$\boldsymbol{L} = \tau_1\boldsymbol{G}(\uparrow)[\tau_3\boldsymbol{G}(\uparrow)]^m\tau_1\boldsymbol{G}(\downarrow)[\tau_3\boldsymbol{G}(\downarrow)]^n\tau_1\boldsymbol{G}(\uparrow)\cdots[\tau_3\boldsymbol{G}(\uparrow)]^p \tag{81}$$

where $m, n, \ldots, p$ are integers. Each $\tau_1\boldsymbol{G}$ is associated with a dark vertex, and each $\tau_3\boldsymbol{G}$ with a light vertex. The trace of $\boldsymbol{L}$ is needed to show that no minus signs attach to spin-up or spin-down propagation directions. It follows from the relations:

$$\tau_3\boldsymbol{G}(\uparrow) = \boldsymbol{G}(\uparrow); \qquad \tau_3\boldsymbol{G}(\downarrow) = -\boldsymbol{G}(\downarrow) \tag{82}$$

and

$$\boldsymbol{G}(\uparrow)^n = i^{n-1}\boldsymbol{G}(\uparrow); \qquad \boldsymbol{G}(\downarrow)^n = (-i)^{n-1}\boldsymbol{G}(\downarrow) \tag{83}$$

that $\boldsymbol{L}$ always reduces to the form:

$$\boldsymbol{L} = i^{m+n+\cdots+p}\tau_1\boldsymbol{G}(\uparrow)\tau_1\boldsymbol{G}(\downarrow)\cdots\tau_1\boldsymbol{G}(\downarrow). \tag{84}$$

Since $\boldsymbol{L}$ by definition has an even number of dark vertices, and since each pair of dark vertices contributes an idempotent matrix via:

$$\tau_1\boldsymbol{G}(\uparrow)\tau_1\boldsymbol{G}(\downarrow) = \begin{pmatrix} 0 & 0 \\ 0 & 1 \end{pmatrix} \tag{85}$$

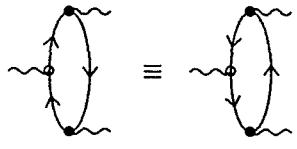

Fig. 2. Equivalent spin propagation loops

one obtains in all cases:

$$\boldsymbol{L} = i^{n+m+\cdots+p}\begin{pmatrix} 0 & 0 \\ 0 & 1 \end{pmatrix}, \quad \text{trace } \boldsymbol{L} = i^{n+m+\cdots+p}. \tag{86}$$

The same signs attach to both spin components, and thus closed loops such as those shown above are equivalent. Each closed fermion loop contributes a minus sign for the reasons established in ordinary many-body theory [21, Appendix 4.A.2]. *No minus signs arise from non-causal propagation lines.*

3.4. Normal diagrams

The excited-state restrictions of Sect. 2.4 are incorporated with the subset of FD described in this section. The labelling scheme is called *normal* to emphasize one-to-one correspondence with the normal starting model.

Normal vertices are in one-to-one correspondence with those of particle-hole theory. At each dark normal vertex, one quasiparticle label must map to a hole label and the other to a particle label. At each light normal vertex, both quasiparticle labels must map to hole labels or both to particle labels.

Normal closed loops are closed loops whose vertices are all normal vertices. Their labels are in one-to-one correspondence with labels for closed loops of the normal problem. Labels that map to particle-labels (hole-labels) of the normal problem are assigned to up-arrows (down-arrows) of normal closed loops.

Normal diagrams are diagrams made up of interaction lines, normal vertices, and normal closed loops. The number of normal diagrams is the same as the number of diagrams for particle-hole theory. The formulae for normal FD are essentially the same as for particle-hole theory.

3.4.1. Energy diagrams. Rules for Goldstone diagrams

(1) For a given order N, draw N interaction lines.

(2) Supply each interaction line with a normal vertex at each end, and draw directed lines, one line into and one line out of each vertex. At each dark vertex, one line must map to a hole line (down-arrow), and the other to a particle line (up-arrow). At each light vertex, both lines must map to hole lines or both to particle lines.

(3) Label each directed line with a quasiparticle label. Use $i, j, k, \ldots,$ $(a, b, c, \ldots,)$ for quasiparticle labels which map to hole (particle) labels of the normal state.

(4) Draw a dotted horizontal line between each successive pair of interaction lines.

(5) Evaluate diagrams by the dictionary of Table 1.

Brandow diagrams. Goldstone diagrams treat direct and exchange interactions separately. Brandow diagrams [23, Appendix B] combine direct and exchange elements into a single antisymmetrized interaction. Brandow diagrams for the present theory combine interactions into a single interaction which is not necessarily an antisymmetrization. The rules may be expressed as modifications of those previously given.

Table 1. Diagram dictionary for ground-state energy (Goldstone diagrams)

Diagram element	Factor
Dotted line:	
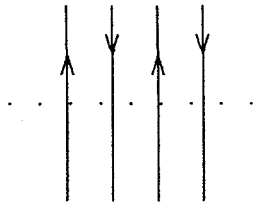	$-1/$(sum of E_q's for all lines crossing dotted line)
Interactions:	
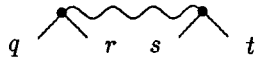	$(\Omega_{qr}\|\Omega_{st})$
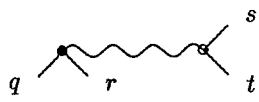	$(\Omega_{qr}\|\Lambda_{st})$
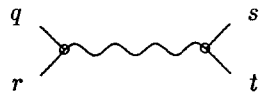	$(\Lambda_{qr}\|\Lambda_{st})$
Each closed loop	-1
Each completely symmetric diagram	$\frac{1}{2}$
Each quasiparticle label q	Σ_q

Rules for Brandow diagrams

(1) Draw just one diagram from the set of all those obtained from each other when direct interactions are replaced by exchange interactions, or vice versa.

(2) Include a factor of $\frac{1}{2}$ for each equivalent pair of lines. Two lines form an equivalent pair if they (a) both begin at the same interaction, (b) both end at the same interaction, and (c) both go in the same direction.

(3) Apart from the entries for interactions and the rule for completely symmetric diagrams, evaluate the diagrams by the dictionary of Table 1. The interaction elements are evaluated by the dictionary of Table 2. The completely symmetric diagrams are covered by the rule for equivalent pairs of lines.

Second and third-order Brandow diagrams. The second-order Brandow diagram is shown on Fig. 3:

$$D^{(2)} = -\sum_{ijab>0} \frac{(\Omega_{ia}|\Omega_{jb})}{D_{iajb}} [2(\Omega_{ai}|\Omega_{bj}) - (\Omega_{aj}|\Omega_{bi})]. \tag{87}$$

Table 2. Dictionary for interaction elements of Brandow diagrams

Element	Factor
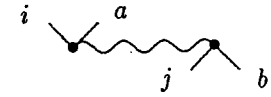	$(\Omega_{ia}\|\Omega_{jb}) - (\Lambda_{ij}\|\Lambda_{ab})$
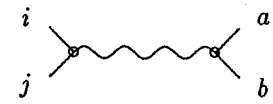	$(\Lambda_{ij}\|\Lambda_{ab}) - (\Omega_{ia}\|\Omega_{jb})$
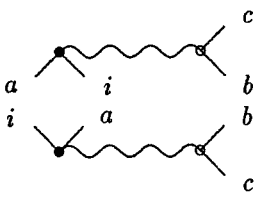	$(\Omega_{ai}\|\Lambda_{bc}) - (\Omega_{bi}\|\Lambda_{ac})$
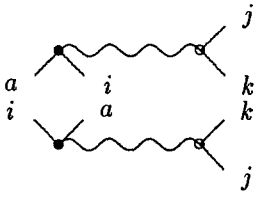	$(\Omega_{ai}\|\Lambda_{jk}) - (\Omega_{ak}\|\Lambda_{ji})$
All others	Antisymmetrized interactions

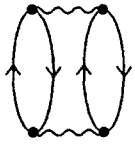

Fig. 3. Second-order Brandow diagram

The symmetric energy denominators are sums of the eigenvalues of Eq. (36) of the uncoupled quasiparticles:

$$D_{qrst} = E_q + E_r + E_s + E_t. \tag{88}$$

Third-order Brandow diagrams are shown on Figs. 4 and 5.

$$\left.\begin{aligned}
D^{(3)}(l_p) &= \sum_{ijabcd>0} \frac{(\Omega_{ia}|\Omega_{jb})}{D_{iajb}} \frac{(\Omega_{ci}|\Omega_{dj})}{D_{cidj}} [2(\Lambda_{ac}|\Lambda_{bd}) - (\Lambda_{ad}|\Lambda_{bc})] \\
D^{(3)}(l_h) &= \sum_{ijklab>0} \frac{(\Omega_{ai}|\Omega_{bj})}{D_{aibj}} \frac{(\Omega_{ka}|\Omega_{lb})}{D_{kalb}} [2(\Lambda_{ik}|\Lambda_{jl}) - (\Lambda_{il}|\Lambda_{jk})] \\
D^{(3)}(r_{ph}) &= 2 \sum_{ijkabc>0} \frac{[2(\Omega_{bk}|\Omega_{ci}) - (\Omega_{bi}|\Omega_{ck})]}{D_{bkci} D_{ijac}} \\
&\quad \times \{[2(\Omega_{ic}|\Omega_{ja}) - (\Omega_{ia}|\Omega_{jc})](\Omega_{aj}|\Omega_{kb}) \\
&\quad + (\Omega_{ka}|\Omega_{jc})(\Lambda_{ab}|\Lambda_{ij}) + (\Omega_{ic}|\Omega_{ja})(\Lambda_{ab}|\Lambda_{kj})\}
\end{aligned}\right\}. \tag{89}$$

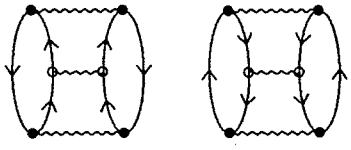

l_p l_h **Fig. 4.** Third-order Brandow ladder diagrams

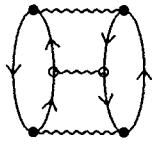

r_{ph} **Fig. 5.** Third-order Brandow ring diagram

The total third-order correction is:

$$D^{(3)} = D^{(3)}(l_p) + D^{(3)}(l_h) + D^{(3)}(r_{ph}). \tag{90}$$

3.5. Diagrammatic formula for total energy

Correlation energy counted by $E^{(1)}$ must not be counted again by finite-order diagrams. For example:

$$E^{(2)} \neq E^{(1)} + D^{(2)} \tag{91}$$

because model FD are counted by $E^{(1)}$ and $D^{(2)}$. Overcount may be corrected up to the order of the theory.

3.5.1. Model scattering diagrams and normal energy. Model scattering diagrams are FD summed to all orders by the unperturbed energy. There are always self-energy summations. Each is associated with a model pair and is labelled by members of the two subsets h_I and p_I in a manner determined by the model. The total contribution from Kth-order model scattering diagrams is the sum of contributions from model pairs:

$$D^{(K)}_{\text{model}} = \sum_I D^{(K)}_{\text{model(I)}}. \tag{92}$$

The first-order energy with model-included FD removed up to the order of the perturbation theory is called the *normal energy*:

$$W^{(N)} = E^{(1)} - \sum_{K=2}^{N} D^{(K)}_{\text{model}}. \tag{93}$$

The total energy is the normal energy plus perturbative corrections:

$$E^{(N)} = W^{(N)} + \sum_{K=2}^{N} D^{(K)}. \tag{94}$$

Equations (93) and (94) are diagrammatic equivalents of discarding the excited state of Eq. (44) discussed in Sect. 2.4.2.

Example: pair scattering. Pair scattering diagrams are model FD for paired quasiparticles. At least two propagator lines carry the same quasiparticle label between successive interaction lines [24, Eq. (15.41)]. Summation limits and ranges for the previous formulae must be modified. Summation limits undergo the replacements:

$$\left.\begin{aligned} i, j, \cdots > 0 &\rightarrow i, j, \cdots \in h_I \\ a, b, \cdots > 0 &\rightarrow a, b, \cdots \in p_I \end{aligned}\right\}. \tag{95}$$

Factors may be inserted in each term of the summations to convert Eqs. (87) and (89) to correlation-energy formulae for pair scattering.

$$\left.\begin{array}{lll} \text{FD} & \text{Factor} & \text{Model pair FD} \\ D^{(2)} & [\delta_{ij}\delta_{ab}] & D^{(2)}_{\text{Pair}(I)} \\ D^{(3)}(l_p) & [\delta_{ab}\delta_{cd}\delta_{ij}] & D^{(3)}_{\text{Pair}(I)}(l_p) \\ D^{(3)}(l_h) & [\delta_{ij}\delta_{kl}\delta_{ab}] & D^{(3)}_{\text{Pair}(I)}(l_h) \\ D^{(3)}(r_{ph}) & [\delta_{ij}\delta_{ik}\delta_{ab}\delta_{ac}] & D^{(3)}_{\text{Pair}(I)}(r_{ph}) \end{array}\right\}. \tag{96}$$

Example: exact scattering. Exact scattering counts all interactions among quasiparticles for a model pair. Summation limits in Eqs. (87) and (89) must be changed according to Eq. (95). No other changes are necessary.

4. Conclusions

A new diagrammatic MBPT is derived, namely BCSLN. The unperturbed problem is defined by a BCS function and modified Hamiltonian. There is no loss of accuracy arising from the violation of particle-number or other conservation principles by the BCS function.

The diagrams of the new method are in one-to-one correspondence with diagrams of particle-hole theory based on a single determinantal unperturbed function, and perturbative calculations with the new method require essentially the same amount of work as particle-hole MBPT. However, the new method is based on a more general unperturbed formulation and its diagrams are well-behaved.

Generation of a perturbative expansion with BCSLN is accomplished with a valency model and adiabatic symmetry correlation diagrams. There is no formal expansion parameter in which to generate a perturbative expansion. Without an expansion parameter there is freedom to write a variety of different exact expressions, each of which yields a different lowest-order approximation. BCSLN must be guided by physics and model calculations which include the relevant contributions to the mean field.

Applications of BCSLN can be carried out with conventional quantum chemical software, and this was exploited in Paper I of this series. GVB [25] was used to compute orbitals, pairing coefficients, and parameters for the model Hamiltonian. A standard 4-index transformation was used to calculate matrix elements for charge distributions. With attention to signs, FD were computed with code from the *Computer Physics* library [26–28]. With this code and the basis sets described in Paper I of this series, the calculations of perturbative corrections through third order for F_2 and N_2 require about 1 min per point on an IBM 3090.

References

1. Pines D (1961) The many-body problem. WA Benjamin, NY
2. Belyaev ST (1968) Collective excitations in nuclei. Gordon and Breach, NY
3. Scadron MD (1979) Advanced quantum theory and its applications through Feynman diagrams. Springer-Verlag, NY
4. Anderson PW (1984) Basic notions of condensed matter physics. Benjamin/Cummings, Menlo Park
5. Blaizot JP, Ripka G (1986) Quantum theory of finite systems. MIT Press, Cambridge
6. Ring P, Schuck P (1980) The nuclear many-body problem. Springer-Verlag, Berlin
7. Nozières P (1964) Theory of interacting Fermi systems. Benjamin, NY
8. Lindgren I, Morrison J (1986) Atomic many-body theory. Springer-Verlag, Berlin
9. England WB, Silver DM (1986) J Chem Phys 85:5847
10. England WB (1982) J Phys Chem 86:1204
11. England WB (1983) Int J Quantum Chem 23:905
12. England WB (1983) Int J Quantum Chem Symp 17:357
13. Sorensen TE, England WB, Silver DM (1986) Int J Quantum Chem Symp 20:81
14. Lipkin HJ (1960) Ann Phys (NY) 9:272
15. England WB, Silver DM, Steinborn EO (1984) J Chem Phys 81:4546
16. Sorensen TE, England WB, Silver DM (1989) J Phys B 22:L539
17. Nogami Y (1964) Phys Rev 134:B313
18. Sorensen TE (1989) Bardeen–Cooper–Schrieffer–Lipkin–Nogami theory: A new method for electronic structure calculations with applications to potential energy curves for H_2, LiH, FH, F_2, and N_2. PhD thesis, Univ of Wisconsin-Milwaukee
19. Rowe DJ (1970) Nuclear collective motion: Models and theory. Methuen, London
20. Sorensen TE, England WB, Silver DM (1992) Quantum field theoretical methods in chemically bonded systems III. BCSLN–HL(N) potential energy curves for the ground states of H_2, LiH, FH and F_2. Theor Chim Acta 84:21–35
21. March NH, Young WH, Sampanthar S (1967) The many-body problem in quantum mechanics. Cambridge Univ Press, London.
22. Schrieffer JR (1964) Theory of superconductivity. WA Benjamin, NY
23. Brandow BH (1967) Rev Mod Phys 39:771
24. Mattuck RD (1976) A guide to Feynman diagrams in the many-body problem. McGraw-Hill, NY
25. Hunt WJ, Hay PJ, Goddard WA (1972) J Chem Phys 57:738
26. Silver DM (1978) Comput Phys Commun 14:71
27. Silver DM (1978) Comput Phys Commun 14:81
28. Wilson S (1978) Comput Phys Commun 14:91